Elsevier Editorial System(tm) for Marine Pollution Bulletin

Manuscript Draft

Manuscript Number: MPB-D-18-00428R1

Title: Petroleum hydrocarbon and microbial community structure successions in marine oil-related aggregates associated with diatoms relevant for Arctic conditions

Article Type: Research Paper

Keywords: oil-related aggregates; biodegradation; diatoms; microbial communities; Arctic

Corresponding Author: Dr. Roman Netzer,

Corresponding Author's Institution: SINTEF Ocean

First Author: Roman Netzer

Order of Authors: Roman Netzer; Ingrid A Henry, PhD; Deni Ribicic, MSc; Daniel Wibberg, PhD; Ute Brönner, MSc; Odd G Brakstad, PhD

Abstract: Oil-related aggregates (ORAs) may contribute to the fate of oil spilled offshore. However, our understanding about the impact of diatoms and associated bacteria involved in the formation of ORAs and the fate of oil compounds in these aggregates is still limited. We investigated these processes in microcosm experiments with defined oil dispersions in seawater at 5°C, employing the Arctic diatom Fragilariopsis cylindrus and its associated bacterial assemblage to promote ORA formation. Accumulation of oil compounds, as well as biodegradation of naphthalenes in ORAs and corresponding water phases, was enhanced in the presence of diatoms. Interestingly, the genus Nonlabens was predominating the bacterial communities in diatom-supplemented microcosms, while this genus was not abundant in other samples. This work elucidates the relevance of diatom biomass for the formation of ORAs, microbial community structures and biodegradation processes in chemically dispersed oil at low temperatures relevant for Arctic conditions.

Petroleum hydrocarbon and microbial community structure successions in marine oil-related aggregates associated with diatoms relevant for Arctic conditions

Roman Netzer*[1], Ingrid A. Henry[1], Deni Ribicic[1], Daniel Wibberg[2], Ute Brönner[1] and Odd G. Brakstad[1]

[1] SINTEF Ocean, Brattørkaia 17C, 7010 Trondheim, Norway

[2] Center for Biotechnology (CeBiTec), Bielefeld University, Universitätsstraße 27, 33615, Bielefeld, Germany

***Corresponding author**: Roman Netzer; e-mail roman.netzer@sintef.no; Phone +47 98230515.

Keywords: oil-related aggregates, biodegradation, diatoms, microbial communities, Arctic

Abstract

Oil-related aggregates (ORAs) may contribute to the fate of oil spilled offshore. However, our understanding about the impact of diatoms and associated bacteria involved in the formation of ORAs and the fate of oil compounds in these aggregates is still limited. We investigated these processes in microcosm experiments with defined oil dispersions in seawater at 5°C, employing the Arctic diatom *Fragilariopsis cylindrus* and its associated bacterial assemblage to promote ORA formation. Accumulation of oil compounds, as well as biodegradation of naphthalenes in ORAs and corresponding water phases, was enhanced in the presence of diatoms. Interestingly, the genus *Nonlabens* was predominating the bacterial communities in diatom-supplemented microcosms, while this genus was not abundant in other samples. This work elucidates the relevance of diatom biomass for the formation of ORAs, microbial community structures and biodegradation processes in chemically dispersed oil at low temperatures relevant for Arctic conditions.

1. Introduction

Marine snow (MS) is formed by natural processes in the oceans and plays a key role in the vertical flux and recycling of particulate and dissolved organic matter (DOM) in the water column (Lombard et al., 2013; Turner, 2002). MS is defined as aggregates ≥ 0.5 mm, composed of organic and inorganic particles such as minerals, detritus, bacteria, mucus, phytoplankton, or zooplankton faeces. The processes involved in MS formation are complex, but both physicochemical mechanisms (e.g. aggregation, coagulation, collision and break-up) and biological actions are suggested to be major contributors (Alldredge and Silver, 1988). Mucus material from various sources, including phyto- and zooplankton, can act as "glue" in the development of MS and bind together separate organic and inorganic constituents into aggregates (Wotton, 2004). This mucus is often termed transparent exopolymer particles (TEP) or extracellular polymeric substances (EPS). Phytoplankton biomass is often a main component of MS, typically dominated by diatoms and coccolithophores (Green et al., 2004; Gutierrez et al., 2013; Gutierrez et al., 2012a; Gutierrez et al., 2012b; Gutierrez et al., 2014). Phytoplankton provides organic material, but also inorganic material, such as calcite (coccolithophores) or silica (diatoms), acting as ballast material and increasing sinking velocities of aggregates due to the high density (Biermann and Engel, 2010; Lombard et al., 2013).

Most hydrocarbon biodegradation experiments in the marine environment have been performed with the free-living bacteria in the seawater, disregarding bacteria adhering to particulate matter and aggregates such as MS (Mishamandani et al., 2016). However, recent studies have revealed that bacteria associated with oil biodegradation are common members of microbial communities in natural MS aggregates, where phytoplankton and prokaryotic microorganisms are closely coexisting in mutually beneficial partnerships (Gutierrez and Aitken, 2014; Gutierrez et al., 2014; Kazamia et al., 2012; Thompson et al., 2017). In addition, oil droplets ingested by zooplankton may generate faecal aggregates, containing bacterial communities able to biodegrade oil (Størdal et al., 2015a; Størdal et al., 2015b). Aggregates of oil, bacteria, EPS and oil degradation products may also be formed during oil biodegradation, in the absence of phytoplankton or zooplankton (Bælum et al., 2012; Hazen et al., 2010). Also, it has been shown that non-polar substances are able to accumulate in the EPS matrix of biofilms (Martirani-Von Abercron et al., 2017). Inorganic material can interact with dispersed oil as oil-mineral aggregates (OMAs), known to cause oil sedimentation (Gong et al., 2014; Lee, 2002; Payne et al., 2003). OMAs form primarily close to riverine outflows,

melting glaciers or sea ice, and in semi-enclosed bays, where suspended lithogenic particle concentrations are relatively high (Lee and Page, 1997; Payne et al., 2003).

The formation and fate of MS related to oil spills gained significant attention after the Deepwater Horizon (DwH) accident in 2010. During the oil spill, ~ 4.1 million barrels of light crude oil and gas were discharged from the Macondo well (MC252) over a period of 87 days. In addition, about 37,000 barrels of the chemical dispersant Corexit were applied on the sea surface and at the well at 1,500 m depth, primarily in order to reduce oil surfacing, improve safety for operating vehicles, and reduce stranding along the shorelines of the Gulf of Mexico (Zukunft, 2010). In oil spill response operations, chemical dispersants can be used to break-up oil-slicks into micron-sized droplets, thereby leading to i) rapid dilution in the water column, that in turn ii) improves biodegradability by providing a readily accessible food source for indigenous oil degrading bacteria without exhausting natural nutrient levels (Lee et al., 2013). The subsurface application of dispersants directly at the well resulted in the formation of a deep-sea plume of small oil droplets. Aggregates of bacteria, polymeric material, oil and oil compound degradation compounds were detected in this plume (Hazen et al., 2010). It was suggested that bacterial blooms driven primarily by consumption of soluble hydrocarbons produced biomass that acted as flocculant to capture suspended hydrocarbon particles and promoted the formation of oily bacterial flocs (Valentine et al., 2014). In addition, surfaced oil was suggested to contribute to MS formation by processes like EPS produced by oil–degrading bacteria (floating biofilms), production of oil particulate matter through interactions of oil components with suspended matter and their coagulation, and coagulation of phytoplankton with oil droplets incorporated into the aggregates (Passow et al., 2012). Different bacteria associated with oil degradation (*Cycloclasticus, Thalassolituus, Marinobacter*) and EPS production (*Halomonas, Pseudoalteromonas, Colwellia, Alteromonas*) have been identified in MS particles (Gutierrez et al., 2013; Suja et al., 2017).

While considerable efforts have been made to investigate MS processes related to the DwH oil spill in the Gulf of Mexico (GoM), only a few studies have focused on oil releases relevant for other areas (Suja et al., 2017). In this study, we investigated the formation of oil-related aggregates as a site for oil biodegradation and microbial community successions at conditions relevant for cold seawater, employing an obligate psychrophilic diatom species, chemically dispersed oil, and natural seawater at low temperature.

2. *Materials and Methods*

2.1. Cultivation of *Fragilariopsis cylindrus*

The obligate psychrophilic diatom *F. cylindrus* RCC 4289 (Roscoff Culture Collection; Station Biologique de Roscoff, Place Georges Teissier, 29680 ROSCOFF Cedex, France) was selected to resemble Arctic algae-bloom conditions. The diatom was grown in L1 medium (nitrate concentration 0.9 mmol/L) with additional silicate (Guillard and Hargraves, 1993). The medium was prepared in natural local seawater and filter sterilized (0.22 µm Millipore filter; Millipore Corporation, Billerica, MA, USA) prior to use. The cultures were grown at 5°C in 250 ml borosilicate flasks (Schott), capped with aluminum foil and random manual agitation, under a 16:8 h light:dark cycle regime (light intensity of 50 µmol photons m^{-2} s^{-1}). Growth was monitored by cell counting using light microscopy at 1,250 times magnification. Cells from the stationary-state phase were used for experimentation.

2.2. Microcosm set-up

Pyrex flasks (2 L; Schott) were used in the experiments. The flasks were pre-treated as previously described (Brakstad et al., 2015), and then filled with natural seawater (acclimatized for 48 h at 5°C), leaving about 50 ml space for adding oil dispersion stock solution (described in section 2.3), diatoms and $HgCl_2$, respectively. Natural seawater was collected from a depth of 80 m (below thermocline) in the Trondheimsfjord (63°26'N, 10°23'E), outside the harbour area of Trondheim. The water is supplied via a pipeline system to our laboratories after passing through a sand filter. Samples amended with oil and diatoms (O+D-samples) contained oil dispersions adjusted to a nominal concentration of 30 mg/L oil droplets (median droplet diameter 9 µm) based on Coulter Counter measurements (see below), while diatoms were added to a final concentration of ~10,000 cells/ml, based on microscopic counting. Oil-amended samples (O-samples) and diatom-amended samples (D-samples) were treated accordingly without diatoms or oil, respectively. Sterilized controls were prepared like O+D-samples and supplemented with 100 mg/L $HgCl_2$. Finally, flasks were filled completely with acclimatized natural seawater to avoid any headspace, sealed tightly and mounted onto a slowly rotating (0.75 rpm) carousel (Brakstad et al., 2015). O+D-, O- and D-samples were prepared in triplicates and incubated in the dark in a temperature-controlled climate room at 4-5°C over a period of 64 days. This temperature is relevant for Arctic surface seawater temperature in the summer season.

2.3. Oil dispersion stock solution

All flocculation experiments were conducted using dispersed fresh Troll C oil (batch 2007-0087) and Corexit 9500A (Nalco). The SINTEF oil droplet generator was used for generating oil dispersion stock solutions with defined droplet size distributions (Nordtug et al., 2015). Oil and dispersant were premixed at room temperature in a dispersant-to-oil ratio (DOR) of 1:100 and injected into a constant flow of filtered (1 µm) and acclimatized natural seawater which moves through a nozzle system, as described elsewhere (Nordtug et al., 2015). A Multisizer 4 Coulter Counter (Beckman Coulter Inc., Brea, CA, USA) fitted with a 100 µm aperture was used to determine oil droplet concentration and size distribution within a diameter range of 2.6 – 60 µm. Filtered (0.22 µm) seawater was used as electrolyte. Median droplet sizes reported here are expressed as median droplet diameter of droplet volume.

2.4. Sampling

Triplicate samples were sacrificed for analysis after 0 (30 min on carousel), 5, 21 and 64 days of incubation. Sterilized controls (one replicate each) were sampled at day 0 and 64. Particles in oil-amended samples with a diameter > 20 µm were defined as oil-related aggregates (ORAs) in the experiments reported here.

Sampling was performed by sacrificing entire bottles at the corresponding sampling time point. Aliquots were taken and subjected to Coulter Counter and dissolved oxygen (DO) analyses (Model 59 Dissolved Oxygen Meter, YSI Inc, Yellow Springs, Ohio, USA). The rest of the sample volume (2.2 L) was filtered through a 20 µm steel filter mesh (Teichhansel Teichshop / Siebgewebeshop; Bockhorn, Germany) using gravimetric force to capture ORAs. Biofilm attached to the glass wall was released by careful shaking prior to filtration. The steel filter was then divided using sterilized scissors and one half of each filter was extracted in 20 ml dichlormethane (DCM) for chemical analyses, while the other half was frozen for subsequent DNA extraction from the ORAs. Planktonic bacteria were collected by filtering 500 ml of the flow-through from the first filtration-step through a 0.22 µm membrane filter by using a vacuum pump. The membrane filter was frozen at -20°C for subsequent DNA extraction. The rest of the flow-through (approximately 1.7 L) was acidified with 15% HCl to pH < 2 and subjected to solvent-solvent extraction with DCM.

2.5. Oil compound analyses

DCM extracts from both the ORAs and the water phases were analyzed by gas chromatographic methods. Total extractable organic material (TEM) analyses were performed

on an Agilent 6890N gas chromatograph with an Agilent 7683B automatic injection system and a flame ionization detector (FID), using He carrier gas and 6890N with Durabond DB-1 column (30m x 0.25mm id, film thickness 0.25 microns). The lower limit of detection (LOD) was 0.1 µg/L with 15% standard deviation.

Quantification of 96 individual targeted compounds in the semivolatile organic carbon (SVOC) fraction included *n*C10-*n*C36 alkanes, decalins, C0-C5 phenols, 2- to 6-ring polycyclic aromatic hydrocarbons (PAH), pristane, phytane and 17α(H),21β(H)-Hopane (30ab hopane), and was performed by GC-MS analyses, as previously described (Brakstad et al., 2014). GC-MS analyses were performed with an Agilent 6890 plus GC coupled with an Agilent 5973 MSD detector, operated in Selected Ion Monitoring (SIM) modus. The gas chromatograph was fitted with a fused silica capillary column (30 or 60 m x 0.25 mm x 0.25 µm film thickness, 5% diphenyl 95% dimethylpolysiloxane stationary phase) and was operated at an initial inlet temperature of 325°C and with He as the carrier gas. Response values for individual target analytes were determined based on a signal-to-noise ratio of > 10, the limit of detection (LOD) was set to 0.01 µg/L for individual oil compounds. For normalization of target compounds, we evaluated the three frequently used biomarker compounds 30ab hopane (Prince et al. 1994), pristane and phytane (Atlas and Bartha 1992). Phytane (2,6,10,14-tetramethylhexadecane) was found to be most persistent under the given conditions with 86.5±13.1% abundance after 64 days incubation and was used for assessing biodegradation of target compounds. In this work, the term biodegradation refers to depletion of analytes normalized with corresponding phytane values.

2.6. Microbial community analysis

DNA from biomass trapped on steel filters (ORAs) and membrane filters (planktonic bacteria) was extracted using the FastDNA Spin kit for soil (MP Biomedicals) in combination with the FastPrep machine (MP Biochemicals), according to the manufacturer's instructions. DNA quantification was performed by Qubit 3.0 fluorometer (Thermo Fisher Scientific Waltham, MA, USA) with dsDNA High Sensitivity kit (ThermoFisher Scientific, MA, USA).

Microbial community composition of the samples collected was analyzed by 16S amplicon sequencing. In brief, 16S rDNA amplicons were generated from DNA-samples by two PCR rounds using the 2x HiFi HotStart ReadyMix (Kapa Biosystems, Boston MA, USA). To amplify the third and fourth variable regions (V3, V4) of the 16S rRNA gene, the primers Pro341F (5'-CCTACGGGNBGCASCAG-3') and Pro805R (5'-GACTACNVGGGTATCT AATCC-3') (Takahashi et al., 2014) covering the domains Bacteria and Archaea were used

for the first PCR round. Sequencing adapters and multiplexing indices where added using the Nextera XT Index kit (Illumina). Following each PCR round, amplicons were purified using the QIAquick PCR purification Kit (Qiagen) and finally the amplicon size and concentration was determined on a BioAnalyzer (Agilent Technologies, Santa Clara, CA, USA). Pooled, normalized DNA libraries (4 pM DNA) were mixed with PhiX (5%) Control v3 (Illumina), denatured at 96°C for 2 minutes and run on a MiSeq sequencer (Illumina) using the MiSeq Reagent Kit v3 in the 2x300bp paired-end mode.

Raw pair-end reads were assembled with fastq-join (Aronesty, 2011) in QIIME 1.9.1 (Caporaso et al., 2010b). Assembled sequences were demultiplexed and quality filtered to remove low quality reads (Phred score < 20; -q 19). UCHIME was employed for chimera detection on assembled quality filtered reads (Edgar et al., 2011). Operational Taxonomic Units (OTUs) were determined by clustering assembled sequences on 97% nucleotide identity using UCLUST (Edgar, 2010) with open reference clustering option. Representative sequences were aligned with PyNAST (Caporaso et al., 2010a), and taxonomy assignment was performed with RDP classifier (Wang et al., 2007), based on SILVA-123 database (Klindworth et al., 2013). To evaluate for potential differences in the dynamics of microbial communities between different samples and sample groups at separate time points, multivariate statistics in the form of principal coordinate analysis (PCoA), based on un-weighted UniFrac distance metrics (Lozupone and Knight, 2005) was carried out. Prior to that, relative abundances of OTUs were calculated, and OTUs with < 0.01% of relative sequence abundance, as well as the OTU based on chloroplast sequences were removed. Statistical analysis was performed within the Phyloseq package v.1.12.2 (McMurdie and Holmes, 2013) in R-studio v.3.2.2. For visualization of taxonomical composition, a cut-off of 5% relative abundance was applied. Taxa failing to meet the cut-off value at any point were assigned to group “Other”.

Nucleotide sequence data were deposited at the European Nucleotide Archive (ENA) under study accession number PRJEB25256.

3. *Results and Discussions* Visual observations and biological activity

In all oil-amended samples, large aggregates were formed during the 64-day incubation period. Samples with 30 mg/L dispersed oil had a homogeneous brown turbidity at sampling days 0 (Fig. S1A) and 5, indicating that oil droplets were evenly dispersed. Nameable formation of visible ORAs was first observed at sampling day 21 (Fig. S1B/B_F). The appearance of ORAs was accompanied by reduced turbidity of the water phases in corresponding samples, which also has been reported by Fu et al. in similar experiments (Fu et al., 2014). Aggregates were found to be larger in samples containing diatoms. Accordingly, more ORA material > 20 µm was captured from O+D-samples than from O-samples by filtration at sampling days 21 and 64 (see Fig. S1B_F and D_F versus Fig. S1C_F and E_F). Visual inspection at day 34 revealed that ORAs in O+D-samples had a more filamentous structure, while ORAs in O-samples had a more compact shape (data not shown). However, no samples were taken, and flasks were not removed from the carousel at that time point to avoid distortion of the microcosms and further experiments are needed for studying structural characteristics during ORA formation in detail. Interestingly, all observed ORAs had a positive buoyancy and were rapidly rising once taken from the carousel, independent of the aggregate size and age. It was somewhat unexpected that the presence of high diatom concentrations in O+D samples did not result in sinking ORAs, indicating that the diatoms alone had not sufficient ballasting effect to counteract the positive buoyancy effect of incorporated oil. However, these observations are in accordance with findings from laboratory studies performed at room temperature in roller-bottles with crude oil and dispersant amended natural seawater (Fu et al., 2014). The authors reported the rapid formation of large flocs within 2 days incubation. Floc size was increasing until day 4 when aggregates started to break into smaller fragments. From day 3, previously sinking flocs began to rise due to incorporation of oil droplets or low-density oil components. The presence of dispersants was found to result in more and smaller flocs. The fact that we in contrast, observed only a few large ORAs is probably caused by less turbulence and rotation in the carousel system compared to the roller-bottle system used by Fu et al. (2014). In general, biodegradation dynamics in aggregates might be influenced by their size and structure. However, due to the fragile and loose structure of ORAs observed in the here reported work, we consider the effect of ORA size on biodegradation of oil compounds and microbial community structures as negligible.

To evaluate biological activity and potential oxygen limitation during the incubation, dissolved oxygen was analyzed in all bottles (Fig. S2). As expected, no oxygen consumption was observed in the sterilized controls, confirming no biological activity over the entire experimental period. Interestingly, also in D-samples with diatoms only, no oxygen consumption was observed. This indicates that bacteria present in the microcosms were not able to proliferate under the given conditions. In all oil-amended samples, a linear depletion of oxygen was observed with slightly faster depletion and lower final O_2 concentrations in O+D- than O-samples. While in O+D-samples 85.0±3.8% O_2 was consumed after 64 days incubation, only 69.5±4.5% O_2 was depleted in O-samples. This suggests that the presence of diatom biomass stimulated biological activity in oil-amended samples.

3.2. Oil compound succession in ORAs and corresponding water phases

3.2.1. Oil droplet concentration and droplet size in the water phase

The initial oil concentration and droplet size was verified in all samples by Coulter Counter measurements at day 0 before the filtration step and was close to the theoretical 30 mg/L and 9 µm, respectively (Fig. S3). In the biological O+D- and O-samples, oil droplet concentrations decreased quickly until day 21. In the sterilized controls, the oil droplet concentration remained stable over the entire incubation period, while the mean particle size increased significantly after 64 days incubation. This may be due to aggregation of oil droplets (and diatoms) by coalescence and absorption to surfaces during incubation and sample processing.

3.2.2. Total extractable semi-volatile hydrocarbon material (TEM)

Analysis of TEM confirmed that initial oil concentrations in oil-amended samples were close to the theoretical 30 mg/L, and over the entire incubation period of 64 days, in total 46.9±3.2% (13.2±1.0 mg/L) and 41.7±11.5% (11.0±3.6 mg/L) of the TEM was depleted in O+D- and O-samples, respectively (Fig. 1). This is distinct less depletion than reported in previous studies, where more than 70% TEM depletion was observed for three different oil dispersions with 3 mg/L oil (Brakstad et al., 2017). However, we cannot exclude that biodegradation was impaired due to low O_2 concentrations and nutrient (i.e. phosphorus, nitrogen) limitation under the tested conditions with 30 mg/L oil towards the end of the experiment (Fig. S2). TEM concentrations in the water phases of oil-amended samples were in accordance with oil droplet concentrations in corresponding samples analyzed by Coulter Counter (Fig. S3A).

To discriminate the fate of oil in ORAs and water phases, aggregates > 20 µm were separated from the water phase by gravimetric filtration through a stainless-steel filter mesh. TEM quantification revealed that at day 0, 97.6±0.3%, 97.1±0.1% and 98% of the TEM was found in the water phases of O+D-samples, O-samples and sterilized controls, respectively (Fig. 1). This confirms that only a negligible fraction of oil droplets adsorbed to the steel filter surface during filtration. Depletion of the TEM in the flow-through after filtration (water phase samples) was reflected by a quick decline in the O+D- and O-samples, and after 64 days of incubation, only 1.5±0.2 mg/L and 2.2±0.9 mg/L TEM were found in the water phase of O+D- and O-samples, corresponding to a depletion of 94.6±0.6% and 91.2±4.3%, respectively. This depletion pattern is in accordance with studies, where biodegradation of chemically dispersed oil at lower concentrations (2-3 mg/L) at 5°C was studied (Brakstad et al., 2018).

The partitioning of TEM between both phases showed that while TEM concentrations were decreasing in the water phase, a simultaneous accumulation occurred in ORAs. TEM accumulation followed a linear succession until day 21, and 73.3±3.7% and 59.8±8.0% of TEM remaining in the sample was detected in ORAs in O+D- and O-samples, respectively. Between sampling day 21 and 64, TEM concentrations in ORAs increased only by 5.5±5.0% and 18.6±8.1% in O+D- and O-samples, respectively (Fig. 1). This is most likely due to biodegradation occurring concomitantly with accumulation of oil compounds, but also saturation effects may have contributed. At sampling day 64, the majority of the remaining TEM was accumulated in the ORAs, with 90.2±0.6% and 85.8±4.1% (corresponding to 13.5±0.7 mg/L and 12.8±1.0 mg/L) in O+D- and O-samples, respectively. In recently reported flocculation experiments with Macondo oil and GoM seawater, it was found that in the presence of diatoms, up to 65% of the carbon in formed aggregates was derived from the added oil (Passow and Ziervogel, 2016), supporting our findings that significant amounts of initially present oil quickly accumulated in ORAs. We also observed minor accumulation of TEM in aggregates in sterilized controls, accompanied with a depletion from the water phases. This was regarded as abiotic processes since the total TEM concentration in these samples was reduced by only 7.7%, and this was most likely due to absorption of oil compounds to surfaces during incubation and sampling (glass wall and filter funnel, respectively), which were not extracted for analysis.

3.2.3. *n*-alkanes

The depletion of semi-volatile *n*-alkanes from the water phases of oil-amended samples was accompanied by an accumulation of *n*-alkanes in ORAs (Fig. S4). In the water phases of O+D- and O-samples, 85.1±2.2% (372.8±45.1 µg/L) and 77.9±3.4% (334.7±34.1 µg/L) of the initially analyzed *n*C14-*n*C30-alkane fraction was depleted already within 21 days of incubation. At the same sampling point, 54.1±4.5% (76.5±11.1 µg/L) and 42.5±7.3% (70.9±18.6 µg/L) of the total *n*-alkane fraction was found to be located in ORAs from O+D- and O-samples, respectively (Fig. S4). These results indicate slightly faster transfer of *n*-alkanes from water phases into ORAs when diatoms were present.

The actual biodegradation of *n*C14-*n*C30-alkanes was assessed by normalizing nominal concentrations with corresponding concentrations of the isoprenoid phytane, as previously described (Douglas et al., 1996; Miget et al., 1969). While depletion from the water phase could be appointed to biodegradation, as well as accumulation in ORAs, depletion of oil compounds in ORAs is suggested to be exclusively caused by biodegradation. In our experiments, no noteworthy depletion of individual *n*C14-*n*C30-alkanes was observed in sterilized controls after 64 days of incubation, confirming no abiotic degradation processes (Fig. S5). Biodegradation of the total *n*-alkane fraction appeared to be faster in ORAs compared to the corresponding water phases, regardless of diatoms being present or not (Fig. 2). At the end of the experiment, the *n*-alkane fractions were found to be similarly biodegraded, with in total 90.6±5.5% and 91.4±7.2% (cumulated ORAs plus water phases) in O+D- and O-samples, respectively. All relative abundances of single *n*C14-*n*C30-alkanes in ORAs and the corresponding water phases of O+D- and O-samples over time are given in Fig. S6. These data show that biotransformation in water phases and ORAs started after sampling day 5, and progressive degradation of all analyzed *n*-alkanes was observed after day 21. At this time point, *n*C14-*n*C20-alkanes were biotransformed 100% and > 72% in ORAs from O+D- and O-samples, respectively (Fig. S6). However, biotransformation of *n*-alkanes > *n*C20 was decelerated with increasing chain length and *n*-alkanes > *n*C21 were still not completely biotransformed after 64 days incubation. These findings are contrary to roller table studies focusing on the effect of high concentrations of Louisiana Sweet Crude oil and Corexit9500 on marine oil snow formation where lower molecular weight *n*-alkanes were found to partition more favorably in MS/MOS than in the aqueous phase (Fu et al., 2014).

Our experiments showed that the formation of ORAs contributed to the depletion of *n*-alkanes from the water phase by a combination of accumulation and biodegradation, and biodegradation was faster in ORAs than in the corresponding water phase. It is worth mentioning, that biodegradation performance was found to be slightly improved in the

presence of diatoms. Since also formation of ORAs was found to be stimulated by diatom biomass, accumulation and biodegradation rates may be correlated.

3.2.4. Aromatic semi-volatile organic compounds (SVOC)

In total, 56 individual semi-volatile aromatic compounds, including naphthalenes, 2- to 6-ring PAHs and decalins were analyzed in the water phases and ORAs from O+D- and O-samples. As seen for the *n*-alkanes (Fig. S4), the summarized concentrations of the SVOC compound groups showed rapid depletion from water phases, accompanied by accumulation in ORAs, occurring even faster in the presence of diatoms (Fig. 3). At sampling day 21, 86.9±4.3% (331.1±21.3 µg/L) of the total SVOC fraction was already depleted from the water phases of O+D-samples, compared to 64.3±6.0% (236.2±32.8 µg/L) depletion in diatom-free O-samples. Notably, after 64 days of incubation, the SVOC fractions in the water phases were similarly depleted with > 95% in both O+D- and O-samples. In accordance, SVOCs accumulated in ORAs until day 21, followed by depletion due to biodegradation after day 21.

However, despite similar depletion from the water phase, biotransformation of the SVOC fractions in the water phase was found to follow different patterns than observed for the *n*-alkane fractions. For example, naphthalene depletion was not accompanied by accumulation in ORAs. In both O+D- and O-samples, only minor accumulation was found during the first five days of incubation, indicating that accumulation and biodegradation occurred simultaneously afterwards (Fig. S7A). Also, in the water phases the naphthalene fraction was biotransformed more rapidly in the presence of diatoms, as 91.1±0.6% was depleted in O+D samples, compared to 63.6±7.5% in diatom-free O-samples at day 21 (Fig. S7B). However, after 64 days of incubation, naphthalenes were equally biotransformed to < 3% in the water phases and < 10% in ORAs regardless if diatoms were present or not. This shows that at an early stage the presence of diatoms enhanced the biotransformation of *n*-alkanes and naphthalenes in the water phase, as well as degradation performance in ORAs. In contrast, degradation of 2-3 ring PAHs, decalins and 4-6 ring PAHs was found to be higher in ORAs derived from diatom-free samples (Fig. S7A). However, biotransformation of these compounds in the corresponding water phases was identical, regardless of the diatoms being present or not (Fig. S7B).

Collectively, SVOC groups were biotransformed in the water phases in decreasing order of naphthalenes > 2-3 ring PAHs > decalins > 4-6 ring PAHs. Analyzing the relative distribution of SVOC groups at individual sampling days revealed a major depletion in the water phases between days 5 and 21, accompanied by simultaneous accumulation in the corresponding ORAs (Fig. 4). After 21 days of incubation, the ORAs of diatom-amended

O+D-samples harbored the majority of the remaining SVOCs (74.5±4.9% decalins, 88.3±3.2% naphthalenes, 79.4±1.7% 2-3 ring PAHs, 74.1±3.9% 4-6 ring PAHs). At the same time, lower percentages of remaining SVOCs were found to be localized in ORAs of diatom-free O-samples (60.1±11.2% decalins, 62.4±9.5% naphthalenes, 55.6±10.3% 2-3 ring PAHs, 59.7±11.6% 4-6 ring PAHs). This indicates that the presence of diatoms enhanced initial SVOC accumulation in ORAs, but overall biotransformation of SVOCs was comparable after 64 days incubation.

3.3. Microbial community structures in ORAs and corresponding water phases

The microbial communities in ORAs and the corresponding water phases of oil-amended O- and O+D-samples, and only diatoms containing D-samples were analyzed by 16S rRNA gene amplicon sequencing, where D-samples served as control to identify dominating taxa associated with the diatom *F. cylindrus*. All samples from the water phases contained sufficient DNA for sequencing at every sampling day (0, 5, 21 and 64), except for ORAs from O-samples at day 5 and diatom aggregates from D-samples at day 0, 5 and 21. See data from each replica in supplementary material table (Tab. S1).

As expected, the microbial communities in ORAs and the corresponding water phases were similar within each treatment but showed differences among the treatments at various sampling days. Principal coordinate analysis (PCoA) revealed that microbial communities in O- and O+D-samples were different at the start of the experiment but became similar during the 64 days of incubation in the ORAs as well as the water phases (Fig. S8). O-samples showed a rich diversity with low abundance < 5% at day 0, constituting 79% and 70% of the identified sequences in the ORAs and water phases, respectively. Over time, this fraction, designated 'Other', became less than 14% at day 64 (Fig. 5). Previous oil biodegradation studies have also shown a typical decrease in microbial diversity accompanied by the emergence of a few dominant oil-degrading microorganisms (Brakstad and Lødeng, 2005).

Analyzing the microbiota at family level revealed that members of *Flavobacteriaceae* (phylum *Bacteriodetes*) were dominant in all samples containing the diatoms but played only a minor role in diatom-free O-samples (Fig. 5). *Flavobacteriaceae* are commonly found in colder marine waters and frequently dominate marine picoplankton communities (Campbell et al., 2015). Members of this family have previously been correlated with degradation of petroleum hydrocarbons and isolated from oil-polluted marine sediments (Dubinsky et al., 2013; Kasai et al., 2002; McFarlin et al., 2017). Since diatoms too have been found in oil-polluted sediments and are known to be capable of hydrocarbon degradation (Paissé et al.,

2008; Prince et al., 2010), it is questionable whether diatoms themselves were responsible for this biodegradation or if hydrocarbons are primarily metabolized by diatom associated oil-degrading bacteria.

Nonlabens, formerly known as *Persicivirga* (Yi and Chun, 2012), was identified as the genus representing *Flavobacteriaceae* in O+D-samples. The relative abundance (RA) of *Nonlabens* in O+D-samples increased dramatically at day 5, comprising 96% and 56% of the identified sequences in ORAs and the corresponding water phases, respectively. Also, massive oxygen depletion in O+D-samples (Fig. S2) indicated that members of this genus were involved in oil degradation. In only diatoms containing D-samples, the initial abundance of 54% reduced to 27% in the ORAs and 2% in the corresponding water phases at day 64, while this bacterium was almost absent in samples containing only oil (O-samples) (Fig. 5). This confirms that the genus *Nonlabens* was closely associated with *F. cylindrus* in our experiments. Algae-bacteria interactions have been previously recognized to play a significant role in biodegradation of crude oil and bioremediation in general (Ramanan et al., 2016; Thompson et al., 2017). To our knowledge, this genus has not yet been associated with hydrocarbon degradation so far. Taken collectively with results from other studies that have described the isolation of novel taxa of oil-degrading bacteria related with marine phytoplankton (Green et al., 2004; Gutierrez and Aitken, 2014; Gutierrez et al., 2013; Gutierrez et al., 2012a; Gutierrez et al., 2012b; Gutierrez et al., 2014), we here hypothesize that *Nonlabens* is a *F. cylindrus* associated genus capable of hydrocarbon degradation. This algal-bacterial association may have potentially profound implications for degradation of spilled oil, in particular under algae-bloom conditions in the Arctic. Even though the yearly primary productivity is low in the Arctic seas and oceans, phytoplankton concentrations may exceed DwH spill concentrations by almost an order of magnitude, as recently highlighted by Vergeynst et al. (2018).

At sampling day 21, the microbial composition in ORAs from O- and O+D-samples showed the largest differences. While ORAs from O-samples were dominated by *Altermonadaceae* (27% RA), *Oceanospirillaceae* (15% RA), *Rhodobacteraceae* (26% RA) and *Sphingomonadaceae* (10% RA), these families played only a minor role in ORAs derived from O+D-samples, which were dominated by *Flavobacteriaceae*, representing 74% RA in the identified microbial community. Most strikingly, *Oleispira* (family *Oceanospirillaceae*) became enriched at day 21 and day 64 in ORAs from both oil treatments, but not in the corresponding water phases. Members of *Oleispira* are able to degrade saturated and unsaturated hydrocarbons and are considered obligate hydrocarbonoclastic bacteria (Brakstad

et al., 2017; Yakimov et al., 2007). This displacement was even more pronounced at family level where the typical oil degrader harboring family *Oceanospirillaceae* was dominant at day 5 in the water phases of oil-amended O- and O+D-samples (70% and 25% RA, respectively), followed by the strong decline to < 2.9% RA in the following sampling points. This early peak in the water phases was also observed in similar experiments with lower oil concentrations (Brakstad et al., 2017). Typically, members of *Colwellia* and *Cycloclasticus* have been associated with biodegradation of aromatic hydrocarbons in oil contaminated marine environments. In our experiments, both genera were detected already at an early stage (from day 5), but only at low abundances (max. 6%). This finding was surprising since it was expected that *Colwelliaceae* and *Piscirickettsiaceae* would become prominent in oil-amended samples at sampling days 21 and 64, as found in the study from Brakstad et al. (2017). *Colwellia* belongs to the order of *Alteromonadales* (Gammaproteobacteria) and members are typically found in cold seawater (Bowman, 2014). However, also the marine oil snow (MOS) floc analysis of Suja et al. (2017) revealed only a very minor fraction of *Colwelliaceae* (< 1%) after 4 weeks incubation with oil. Suja et al. studied the microbial response towards crude oil with dispersant at subarctic conditions, by analysing the bacterial community in MOS and the surrounding seawater after 2.5 and 4 weeks. Within the floc, *Alcanivoracaceae*, *Alteromonadaceae* and *Pseudoalteromonadaceae* were the dominant members (> 25%) of the MOS community. *Rhodobacteraceae*, *Rhodospirillaceae*, *Vibrionaceae* and *Piscirickettsiaceae* were abundant below 3%, which was in strong contrast to the surrounding seawater dominated by *Vibrionaceae* (46.1%) (Suja et al., 2017).

Interestingly, the microbial composition of ORAs became quite similar at family level at day 64. In fact, at day 64, ORAs from only diatoms containing samples (D-samples) were also dominated by *Alteromonadacea*, *Flavobacteriaceae*, *Oceanospirillaceae* and *Rhodobacteraceae*, which is very similar to the oil-amended O- and O+D-samples (Fig. 5). *Rhodobacteraceae* (Alphaproteobacteria) were clearly linked to oil degradation and reached the maximum abundance in O-samples at day 21 with 76% in the water phase and 26% in ORAs. In O+D-samples, the maximum abundance occurred later at day 64 with a similar distribution in the water phase and ORAs (46% and 36%, respectively). Since *Rhodobacteraceae* were found in D-samples at day 0, this family might have been associated with the diatom *F. cylindrus*. The family *Rhodobacteraceae* includes the marine *Roseobacter* group, which is also known to contain members closely associated with algae ubiquitously (Ramanan et al., 2016). The *Roseobacter clade NAC11-7 lineage* was only found dominant in

493 the presence of oil, at slightly higher abundance in ORAs than in the corresponding water
494 phases (see Fig. 5).
495 During our study, the relative abundance of the gammaproteobacterial *Marinobacter* was
496 very low in the water phases (< 4%), while a maximum abundance of 14% was found in
497 aggregates of oil-free D-samples at day 64. Interestingly, this genus was not detected above
498 0.1% RA in oil-amended O- and O+D-samples. This contrasts with the increase of
499 *Marinobacter* in MOS from 2.5 weeks and 4 weeks that was observed by Suja et al. (2017).
500 This hydrocarbonoclastic genus is known to produce EPS and therefore readily isolated from
501 marine aggregates, but also from oil wells, since many members are capable of alkane
502 degradation and can be enriched by marine oil spill contamination (Arnosti et al., 2016).
503 Members of this genus have previously been identified to live in close association with
504 diatoms (Mishamandani et al., 2016). Our experiment indicates that *Marinobacter* was a
505 member of the *F. cylindrus* associated bacterial community, but at considerable low
506 abundance.
507 Interestingly, members of the family *Sphingomonadaceae* (Alphaproteobacteria) became
508 abundant in O-samples at day 21 and 64 in the ORAs (10% and 17%, respectively) and water
509 phases (5% and 24%, respectively), while in samples containing oil and diatoms together, the
510 maximum relative abundance was < 4% at day 64. This late succession could be linked to the
511 ability of *Sphingomonadaceae* to degrade high molecular weight PAHs (Ghosal et al., 2016).
512 It has to be mentioned that the observed oxygen depletion in O+D- and O-samples
513 towards the end of the experiment may have enhanced the formation of anoxic zones in
514 ORAs, as microelectrode studies have revealed that oxygen can become depleted in marine
515 snow or sinking algal aggregates (Bianchi et al., 2018; Bristow, 2018; Kamp et al., 2016;
516 Ploug et al., 1997; Stief et al., 2016). In particles ≥ 1mm, anoxic micro-niches may even occur
517 when the bulk fluid is saturated with oxygen (Klawonn et al., 2015). ORAs in this study
518 harbored the strictly aerobic *Nonlabens* (Yi and Chun, 2012), but also facultatively anaerobic
519 bacteria such as *Oleispira* (Yakimov et al., 2003), *Colwellia* (Stal, 2016),
520 *Sphingomonadaceae* (Glaeser and Kämpfer, 2014) and *Marinobacter* (Gao et al., 2013) were
521 abundant at day 64. In our experiments *n*-alkanes and SVOCs were largely depleted at day 21
522 prior to oxygen limitation, indicating that anaerobic biodegradation played a negligible role.
523 However, future studies of larger aggregates should consider exploring anoxic
524 microenvironments and their role in biodegradation.
525 In summary, microbiome profiling revealed that bacterial communities in diatom-
526 amended O+D- and D-samples were dominated by algae-associated bacteria of the genus

Nonlabens, and significantly different from communities in diatom-free O-samples, which were dominated by well-known oil degrading genera. However, chemical analysis showed that oil biodegradation performance was not reduced but rather slightly improved in the presence of diatoms. We therefore propose that the diatom-associated bacterial communities possess potent hydrocarbonoclastic capabilities and genus *Nonlabens* harbours oil-degrading species. In contrast, microbial community structures were similar in ORAs and corresponding water phases. Still, abundancies of the individual taxa varied, and certain families became more abundant in ORAs (e.g. *Oceanospirillaceae* and *Colwelliaceae*), while others were more abundant in the water phases (e.g. *Rhodobacteraceae*).

4. Conclusions

The here presented work describes for the first time the impact of Arctic diatoms on biodegradation of dispersed oil, as well as the accompanied microbial community structure dynamics, in oil-related aggregates (ORAs) and the surrounding water phase at conditions relevant for an Arctic environment. The observed differences in the morphology of ORAs at an intermediate phase were most likely related to the presence of diatoms. However, no systematic difference was found after 64 days incubation. Formation of ORAs contributed to the depletion of *n*-alkanes from the water phase by a combination of accumulation and biodegradation. Nevertheless, there was no significant difference in *n*-alkane biodegradation in ORAs and corresponding water phases derived from O+D- and O-samples. It is notable, that biodegradation performance was found to be slightly improved in the presence of diatoms. No biodegradation of SVOCs was found in oil-amended samples derived ORAs and corresponding water phases until sampling day 5. Until then, depletion in the water phases was mainly due to accumulation in ORAs. After the 5 days lag phase, rapid biodegradation of naphthalenes was observed in ORAs and water phases of oil-amended samples, followed by degradation of 2-3 ring PAHs from day 21, and at a lower extend also decalins and 4-6 ring PAHs. The presence of diatoms stimulated the formation of ORAs accompanied by increased accumulation of hydrocarbons, resulting in enhanced removal of hydrocarbons from corresponding water phases. Microbial community structure analyses identified *Nonlabens* as pre-dominant bacterial genus in diatom-amended samples. Persistent dominance in O+D- samples in combination with oil biodegradation performance similar to algae-free samples indicates that members of this genus are potent hydrocarbon degraders.

Chemically dispersed oil was used in the current study, and the large surfaces generated by the small oil droplets facilitated the generation of ORAs. Although lower oil concentrations

were used in the here presented work than in most other reported studies on this subject, dispersant treatment of oil spills results in rapid dilution of the oil (Lee et al., 2013), and whether ORA formation is an important process after dispersant treatment, has not been clarified. Further studies are therefore needed to characterize ORA formation and fate at very low oil concentrations.

Acknowledgements

The research described in this paper was funded by Statoil Petroleum. We would like to thank Marianne Unaas Rønsberg, Inger K. Almås, Marianne Aas, Kristin Bonaunet and Inger Steinsvik for chemical analyses and experimental assistance. Bioinformatics support by the BMBF-funded project "Bielefeld-Gießen Center for Microbial Bioinformatics - BiGi (Grant Number 031A533)" within the German Network for Bioinformatics Infrastructure (de.NBI) is gratefully acknowledged.

5. *References*

Alldredge, A.L., Silver, M.W., 1988. Characteristics, dynamics and significance of marine snow. Progress in Oceanography 20, 41-82.

Arnosti, C., Ziervogel, K., Yang, T., Teske, A., 2016. Oil-derived marine aggregates–hot spots of polysaccharide degradation by specialized bacterial communities. Deep Sea Research Part II: Topical Studies in Oceanography 129, 179-186.

Aronesty, E., 2011. ea-utils: Command-line tools for processing biological sequencing data. Durham, NC: Expression Analysis.

Bianchi, D., Weber, T.S., Kiko, R., Deutsch, C., 2018. Global niche of marine anaerobic metabolisms expanded by particle microenvironments. Nature Geoscience 11, 263-268.

Biermann, A., Engel, A., 2010. Effect of CO2 on the properties and sinking velocity of aggregates of the coccolithophore Emiliania huxleyi. Biogeosciences 7, 1017-1029.

Bowman, J.P., 2014. The family colwelliaceae. The Prokaryotes: Gammaproteobacteria, 179-195.

Brakstad, O.G., Lødeng, A.G.G., 2005. Microbial Diversity during Biodegradation of Crude Oil in Seawater from the North Sea. Microbial Ecology 49, 94-103.

Brakstad, O.G., Nordtug, T., Throne-Holst, M., 2015. Biodegradation of dispersed Macondo oil in seawater at low temperature and different oil droplet sizes. Marine pollution bulletin 93, 144-152.

Brakstad, O.G., Ribicic, D., Winkler, A., Netzer, R., 2017. Biodegradation of dispersed oil in seawater is not inhibited by a commercial oil spill dispersant. Marine Pollution Bulletin.

Bristow, L.A., 2018. Anoxia in the snow. Nature Geoscience 11, 226-227.

Bælum, J., Borglin, S., Chakraborty, R., Fortney, J.L., Lamendella, R., Mason, O.U., Auer, M., Zemla, M., Bill, M., Conrad, M.E., 2012. Deep-sea bacteria enriched by oil and dispersant from the Deepwater Horizon spill. Environmental microbiology 14, 2405-2416.

Campbell, A.M., Fleisher, J., Sinigalliano, C., White, J.R., Lopez, J.V., 2015. Dynamics of marine bacterial community diversity of the coastal waters of the reefs, inlets, and wastewater outfalls of southeast Florida. MicrobiologyOpen 4, 390-408.

Caporaso, J., Bittinger, K., Bushman, F., Desantis, T., Andersen, G., Knight, R., 2010a. PyNAST: a flexible tool for aligning sequences to a template alignment. Bioinformatics 26, 266e267.

Caporaso, J.G., Kuczynski, J., Stombaugh, J., Bittinger, K., Bushman, F.D., Costello, E.K., Fierer, N., Pena, A.G., Goodrich, J.K., Gordon, J.I., 2010b. QIIME allows analysis of high-throughput community sequencing data. Nature methods 7, 335.

Douglas, G.S., Bence, A.E., Prince, R.C., McMillen, S.J., Butler, E.L., 1996. Environmental Stability of Selected Petroleum Hydrocarbon Source and Weathering Ratios. Environmental Science & Technology 30, 2332-2339.

607 Dubinsky, E.A., Conrad, M.E., Chakraborty, R., Bill, M., Borglin, S.E., Hollibaugh, J.T., Mason,
608 O.U., M. Piceno, Y., Reid, F.C., Stringfellow, W.T., Tom, L.M., Hazen, T.C., Andersen, G.L.,
609 2013. Succession of Hydrocarbon-Degrading Bacteria in the Aftermath of the Deepwater
610 Horizon Oil Spill in the Gulf of Mexico. Environmental Science & Technology 47, 10860-
611 10867.
612 Edgar, R.C., 2010. Search and clustering orders of magnitude faster than BLAST. Bioinformatics 26,
613 2460-2461.
614 Edgar, R.C., Haas, B.J., Clemente, J.C., Quince, C., Knight, R., 2011. UCHIME improves sensitivity
615 and speed of chimera detection. Bioinformatics 27, 2194-2200.
616 Fu, J., Gong, Y., Zhao, X., O'Reilly, S.E., Zhao, D., 2014. Effects of oil and dispersant on formation of
617 marine oil snow and transport of oil hydrocarbons. Environmental science & technology 48,
618 14392-14399.
619 Gao, W., Cui, Z., Li, Q., Xu, G., Jia, X., Zheng, L., 2013. Marinobacter nanhaiticus sp. nov.,
620 polycyclic aromatic hydrocarbon-degrading bacterium isolated from the sediment of the South
621 China Sea. Antonie van Leeuwenhoek 103, 485-491.
622 Ghosal, D., Ghosh, S., Dutta, T.K., Ahn, Y., 2016. Current State of Knowledge in Microbial
623 Degradation of Polycyclic Aromatic Hydrocarbons (PAHs): A Review. Frontiers in
624 Microbiology 7, 1369.
625 Glaeser, S.P., Kämpfer, P., 2014. The Family Sphingomonadaceae, in: Rosenberg, E., DeLong, E.F.,
626 Lory, S., Stackebrandt, E., Thompson, F. (Eds.), The Prokaryotes: Alphaproteobacteria and
627 Betaproteobacteria. Springer Berlin Heidelberg, Berlin, Heidelberg, pp. 641-707.
628 Gong, Y., Zhao, X., Cai, Z., O'Reilly, S.E., Hao, X., Zhao, D., 2014. A review of oil, dispersed oil and
629 sediment interactions in the aquatic environment: Influence on the fate, transport and
630 remediation of oil spills. Marine Pollution Bulletin 79, 16-33.
631 Green, D.H., Llewellyn, L.E., Negri, A.P., Blackburn, S.I., Bolch, C.J.S., 2004. Phylogenetic and
632 functional diversity of the cultivable bacterial community associated with the paralytic
633 shellfish poisoning dinoflagellate Gymnodinium catenatum. FEMS Microbiology Ecology 47,
634 345-357.
635 Guillard, R.R.L., Hargraves, P.E., 1993. Stichocrysis immobilis is a diatome, not a chyrsophyte.
636 Phycologia 32, 234-236.
637 Gutierrez, T., Aitken, M.D., 2014. Role of methylotrophs in the degradation of hydrocarbons during
638 the Deepwater Horizon oil spill. ISME J 8, 2543-2545.
639 Gutierrez, T., Berry, D., Yang, T.T., Mishamandani, S., McKay, L., Teske, A., Aitken, M.D., 2013.
640 Role of Bacterial Exopolysaccharides (EPS) in the Fate of the Oil Released during the
641 Deepwater Horizon Oil Spill. Plos One 8.
642 Gutierrez, T., Green, D.H., Whitman, W.B., Nichols, P.D., Semple, K.T., Aitken, M.D., 2012a.
643 Algiphilus aromaticivorans gen. nov., sp. nov., an aromatic hydrocarbon-degrading bacterium

644 isolated from a culture of the marine dinoflagellate Lingulodinium polyedrum, and proposal of
645 Algiphilaceae fam. nov. International journal of systematic and evolutionary microbiology 62,
646 2743-2749.
647 Gutierrez, T., Nichols, P.D., Whitman, W.B., Aitken, M.D., 2012b. Porticoccus hydrocarbonoclasticus
648 sp. nov., an aromatic hydrocarbon-degrading bacterium identified in laboratory cultures of
649 marine phytoplankton. Applied and environmental microbiology 78, 628-637.
650 Gutierrez, T., Rhodes, G., Mishamandani, S., Berry, D., Whitman, W.B., Nichols, P.D., Semple, K.T.,
651 Aitken, M.D., 2014. Polycyclic aromatic hydrocarbon degradation of phytoplankton-
652 associated Arenibacter spp. and description of Arenibacter algicola sp. nov., an aromatic
653 hydrocarbon-degrading bacterium. Applied and environmental microbiology 80, 618-628.
654 Hazen, T.C., Dubinsky, E.A., DeSantis, T.Z., Andersen, G.L., Piceno, Y.M., Singh, N., Jansson, J.K.,
655 Probst, A., Borglin, S.E., Fortney, J.L., Stringfellow, W.T., Bill, M., Conrad, M.E., Tom,
656 L.M., Chavarria, K.L., Alusi, T.R., Lamendella, R., Joyner, D.C., Spier, C., Baelum, J., Auer,
657 M., Zemla, M.L., Chakraborty, R., Sonnenthal, E.L., D'haeseleer, P., Holman, H.Y.N.,
658 Osman, S., Lu, Z.M., Van Nostrand, J.D., Deng, Y., Zhou, J.Z., Mason, O.U., 2010. Deep-Sea
659 Oil Plume Enriches Indigenous Oil-Degrading Bacteria. Science 330, 204-208.
660 Kamp, A., Stief, P., Bristow, L.A., Thamdrup, B., Glud, R.N., 2016. Intracellular Nitrate of Marine
661 Diatoms as a Driver of Anaerobic Nitrogen Cycling in Sinking Aggregates. Frontiers in
662 Microbiology 7, 1669.
663 Kasai, Y., Kishira, H., Harayama, S., 2002. Bacteria belonging to the genus cycloclasticus play a
664 primary role in the degradation of aromatic hydrocarbons released in a marine environment.
665 Applied and environmental microbiology 68, 5625-5633.
666 Kazamia, E., Czesnick, H., Nguyen, T.T.V., Croft, M.T., Sherwood, E., Sasso, S., Hodson, S.J.,
667 Warren, M.J., Smith, A.G., 2012. Mutualistic interactions between vitamin B12-dependent
668 algae and heterotrophic bacteria exhibit regulation. Environmental Microbiology 14, 1466-
669 1476.
670 Klawonn, I., Bonaglia, S., Brüchert, V., Ploug, H., 2015. Aerobic and anaerobic nitrogen
671 transformation processes in N 2-fixing cyanobacterial aggregates. The ISME journal 9, 1456.
672 Klindworth, A., Pruesse, E., Schweer, T., Peplies, J., Quast, C., Horn, M., Glöckner, F.O., 2013.
673 Evaluation of general 16S ribosomal RNA gene PCR primers for classical and next-generation
674 sequencing-based diversity studies. Nucleic Acids Research 41, e1-e1.
675 Lee, K., 2002. Oil-particle interactions in aquatic environments: Influence on the transport, fate, effect
676 and remediation of oil spills. Spill Science & Technology Bulletin 8, 3-8.
677 Lee, K., Nedwed, T., Prince, R.C., Palandro, D., 2013. Lab tests on the biodegradation of chemically
678 dispersed oil should consider the rapid dilution that occurs at sea. Marine Pollution Bulletin
679 73, 314-318.

Lee, R.F., Page, D.S., 1997. Petroleum hydrocarbons and their effects in subtidal regions after major oil spills. Marine Pollution Bulletin 34, 928-940.

Lombard, F., Guidi, L., Kiorboe, T., 2013. Effect of type and concentration of ballasting particles on sinking rate of marine snow produced by the appendicularian Oikopleura dioica. PLoS One 8, e75676.

Lozupone, C., Knight, R., 2005. UniFrac: a new phylogenetic method for comparing microbial communities. Applied and environmental microbiology 71, 8228-8235.

Martirani-Von Abercron, S.-M., Marín, P., Solsona-Ferraz, M., Castañeda-Cataña, M.-A., Marqués, S., 2017. Naphthalene biodegradation under oxygen-limiting conditions: community dynamics and the relevance of biofilm-forming capacity. Microbial Biotechnology 10, 1781-1796.

McFarlin, K.M., Questel, J.M., Hopcroft, R.R., Leigh, M.B., 2017. Bacterial community structure and functional potential in the northeastern Chukchi Sea. Continental Shelf Research 136, 20-28.

McMurdie, P.J., Holmes, S., 2013. phyloseq: an R package for reproducible interactive analysis and graphics of microbiome census data. PloS one 8, e61217.

Miget, R.J., Oppenheimer, C.H., Kator, H.I., LaRock, P.A., 1969. Microbial Degradation Of Normal Paraffin Hydrocarbons In Crude Oil. International Oil Spill Conference Proceedings 1969, 327-331.

Mishamandani, S., Gutierrez, T., Berry, D., Aitken, M.D., 2016. Response of the bacterial community associated with a cosmopolitan marine diatom to crude oil shows a preference for the biodegradation of aromatic hydrocarbons. Environmental Microbiology 18, 1817-1833.

Nordtug, T., Olsen, A.J., Salaberria, I., Øverjordet, I.B., Altin, D., Størdal, I.F., Hansen, B.H., 2015. Oil droplet ingestion and oil fouling in the copepod Calanus finmarchicus exposed to mechanically and chemically dispersed crude oil. Environmental toxicology and chemistry 34, 1899-1906.

Paissé, S., Coulon, F., Goñi-Urriza, M., Peperzak, L., McGenity, T.J., Duran, R., 2008. Structure of bacterial communities along a hydrocarbon contamination gradient in a coastal sediment. FEMS Microbiology Ecology 66, 295-305.

Passow, U., Ziervogel, K., 2016. Marine Snow Sedimented Oil Released During the Deepwater Horizon Spill. Oceanography 29, 118-125.

Passow, U., Ziervogel, K., Asper, V., Diercks, A., 2012. Marine snow formation in the aftermath of the Deepwater Horizon oil spill in the Gulf of Mexico. Environmental Research Letters 7, 035301.

Payne, J.R., Clayton, J.R., Kirstein, B.E., 2003. Oil/Suspended Particulate Material Interactions and Sedimentation. Spill Science & Technology Bulletin 8, 201-221.

Ploug, H., Kühl, M., Buchholz-Cleven, B., Jørgensen, B.B., 1997. Anoxic aggregates - an ephemeral phenomenon in the pelagic environment? Aquatic Microbial Ecology 13, 285-294.

716 Prince, R., Gramain, A., McGenity, T.J., 2010. Prokaryotic hydrocarbon degraders, Handbook of
717 hydrocarbon and lipid microbiology. Springer, pp. 1669-1692.
718 Ramanan, R., Kim, B.-H., Cho, D.-H., Oh, H.-M., Kim, H.-S., 2016. Algae–bacteria interactions:
719 Evolution, ecology and emerging applications. Biotechnology Advances 34, 14-29.
720 Stal, L.J., 2016. The Marine Microbiome: An Untapped Source of Biodiversity and Biotechnological
721 Potential, in: Stal, L.J., Cretoiu, M.S. (Eds.). Springer International Publishing : Imprint:
722 Springer.
723 Stief, P., Kamp, A., Thamdrup, B., Glud, R.N., 2016. Anaerobic Nitrogen Turnover by Sinking
724 Diatom Aggregates at Varying Ambient Oxygen Levels. Frontiers in Microbiology 7, 98.
725 Størdal, I.F., Olsen, A.J., Jenssen, B.M., Netzer, R., Altin, D., Brakstad, O.G., 2015a.
726 Biotransformation of petroleum hydrocarbons and microbial communities in seawater with oil
727 dispersions and copepod feces. Marine pollution bulletin 101, 686-693.
728 Størdal, I.F., Olsen, A.J., Jenssen, B.M., Netzer, R., Hansen, B.H., Altin, D., Brakstad, O.G., 2015b.
729 Concentrations of viable oil-degrading microorganisms are increased in feces from Calanus
730 finmarchicus feeding in petroleum oil dispersions. Marine pollution bulletin 98, 69-77.
731 Suja, L.D., Summers, S., Gutierrez, T., 2017. Role of EPS, Dispersant and Nutrients on the Microbial
732 Response and MOS Formation in the Subarctic Northeast Atlantic. Frontiers in Microbiology
733 8, 676.
734 Takahashi, S., Tomita, J., Nishioka, K., Hisada, T., Nishijima, M., 2014. Development of a
735 prokaryotic universal primer for simultaneous analysis of bacteria and archaea using next-
736 generation sequencing. PloS one 9, e105592.
737 Thompson, H., Angelova, A., Bowler, B., Jones, M., Gutierrez, T., 2017. Enhanced crude oil
738 biodegradative potential of natural phytoplankton-associated hydrocarbonoclastic bacteria.
739 Environ Microbiol 19, 2843-2861.
740 Turner, J.T., 2002. Zooplankton fecal pellets, marine snow and sinking phytoplankton blooms.
741 Aquatic microbial ecology 27, 57-102.
742 Valentine, D.L., Fisher, G.B., Bagby, S.C., Nelson, R.K., Reddy, C.M., Sylva, S.P., Woo, M.A., 2014.
743 Fallout plume of submerged oil from Deepwater Horizon. Proc Natl Acad Sci U S A 111,
744 15906-15911.
745 Vergeynst, L., Wegeberg, S., Aamand, J., Lassen, P., Gosewinkel, U., Fritt-Rasmussen, J., Gustavson,
746 K., Mosbech, A., 2018. Biodegradation of marine oil spills in the Arctic with a Greenland
747 perspective. Science of The Total Environment 626, 1243-1258.
748 Wang, Q., Garrity, G.M., Tiedje, J.M., Cole, J.R., 2007. Naive Bayesian classifier for rapid
749 assignment of rRNA sequences into the new bacterial taxonomy. Applied and environmental
750 microbiology 73, 5261-5267.
751 Wotton, R.S., 2004. The ubiquity and many roles of exopolymers (EPS) in aquatic systems Sci. Mar.
752 68, 13-21.

753 Yakimov, M.M., Giuliano, L., Gentile, G., Crisafi, E., Chernikova, T.N., Abraham, W.-R., Lünsdorf,
754 H., Timmis, K.N., Golyshin, P.N., 2003. Oleispira antarctica gen. nov., sp. nov., a novel
755 hydrocarbonoclastic marine bacterium isolated from Antarctic coastal sea water. International
756 Journal of Systematic and Evolutionary Microbiology 53, 779-785.
757 Yakimov, M.M., Timmis, K.N., Golyshin, P.N., 2007. Obligate oil-degrading marine bacteria. Current
758 Opinion in Biotechnology 18, 257-266.
759 Yi, H., Chun, J., 2012. Unification of the genera Nonlabens, Persicivirga, Sandarakinotalea and
760 Stenothermobacter into a single emended genus, Nonlabens, and description of Nonlabens
761 agnitus sp. nov. Systematic and Applied Microbiology 35, 150-155.
762 Zukunft, P.F., 2010. Summary Report for SubSea and SubSurface Oil and Dispersant Detection:
763 Sampling and Monitoring. [U.S. Department of Homeland Security, U.S. Coast Guard],
764 Operational Science Advisory Team (OSAT), Unified Area Command.

765

Figures

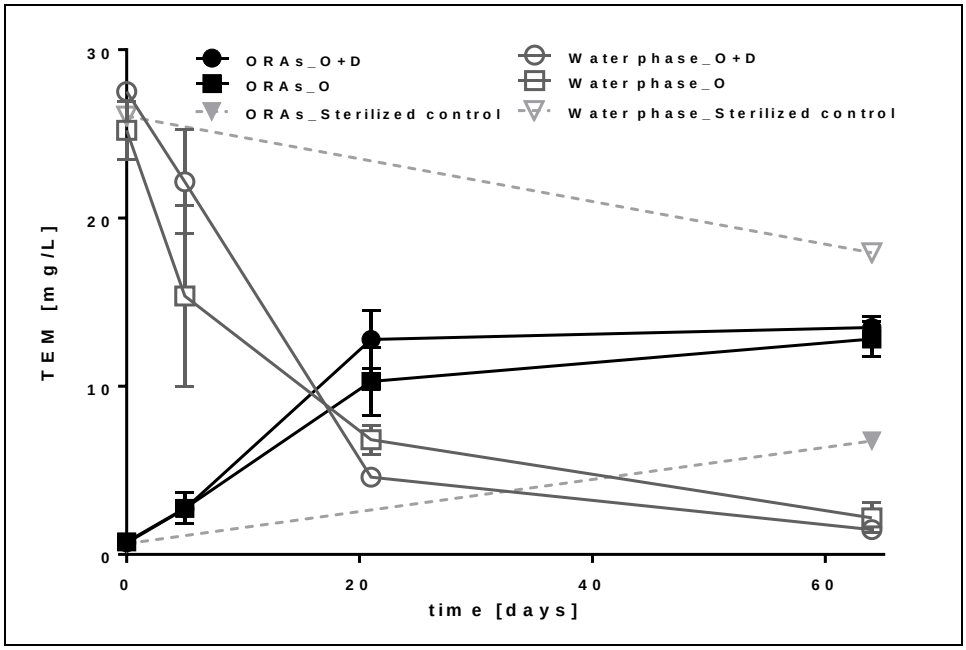

Fig. 1: *Succession of TEM concentrations in the ORAs and water phases of O+D- (oil + diatoms) samples, O- (oil) samples and sterilized controls (sterilized O+D-samples) over the incubation time.*

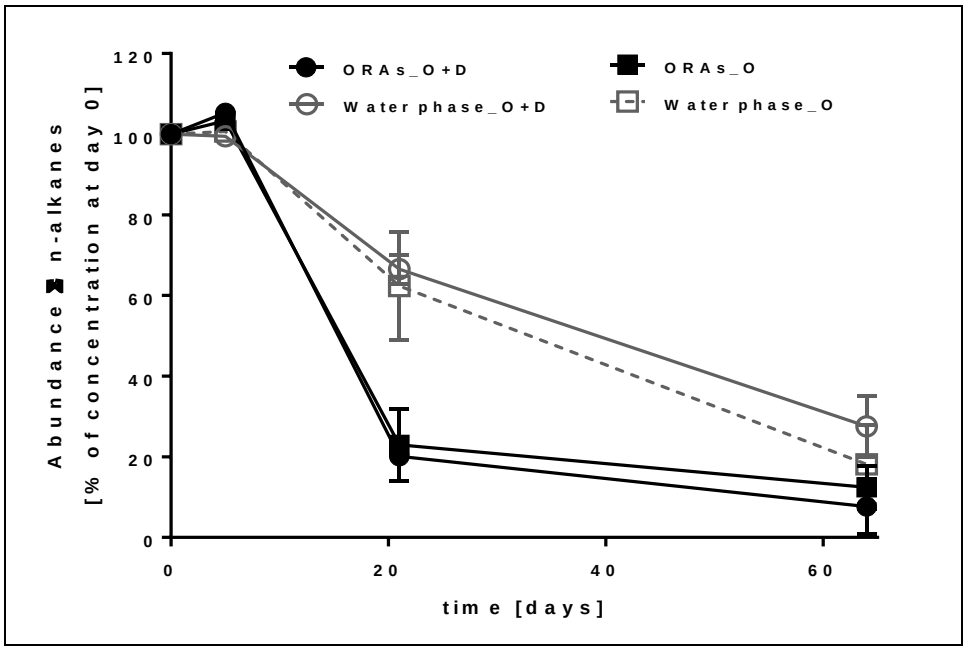

Fig. 2: *Abundance (phytane normalized concentrations) of nC14-nC30-alkane fraction in the ORAs and water phases of O+D- (oil + diatoms) samples and O- (oil) samples over the incubation time.*

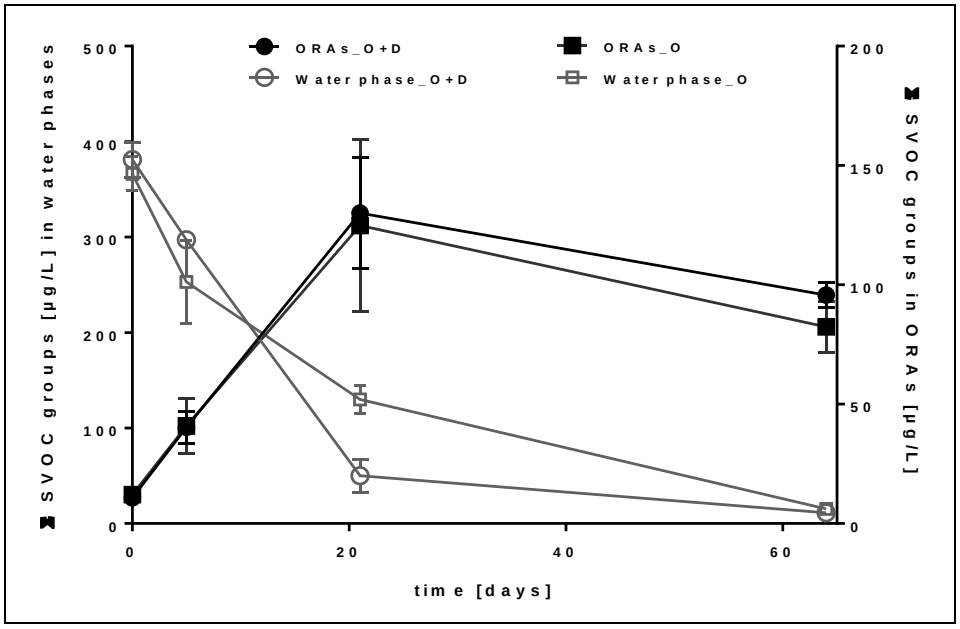

Fig. 3: *Concentrations of summarized SVOC groups over time in ORAs and water phases of O+D- (oil + diatoms) samples and O- (oil) samples over the incubation time. Note the difference in scaling of the water phases and ORAs.*

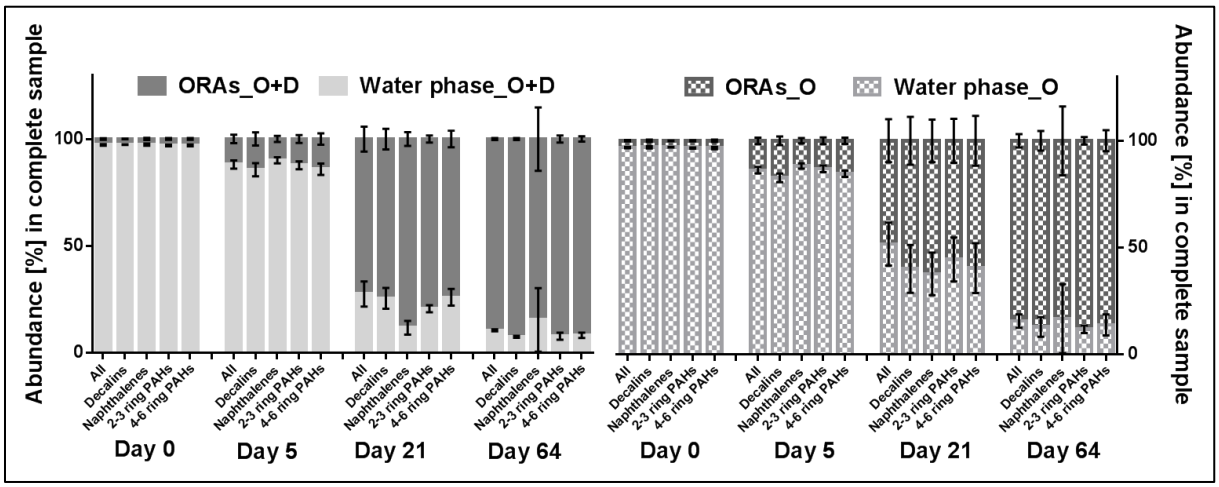

Fig. 4: *Relative distribution of SVOC groups between ORAs and water phases of O+D- (oil + diatoms) samples and O- (oil) samples at the different sampling days.*

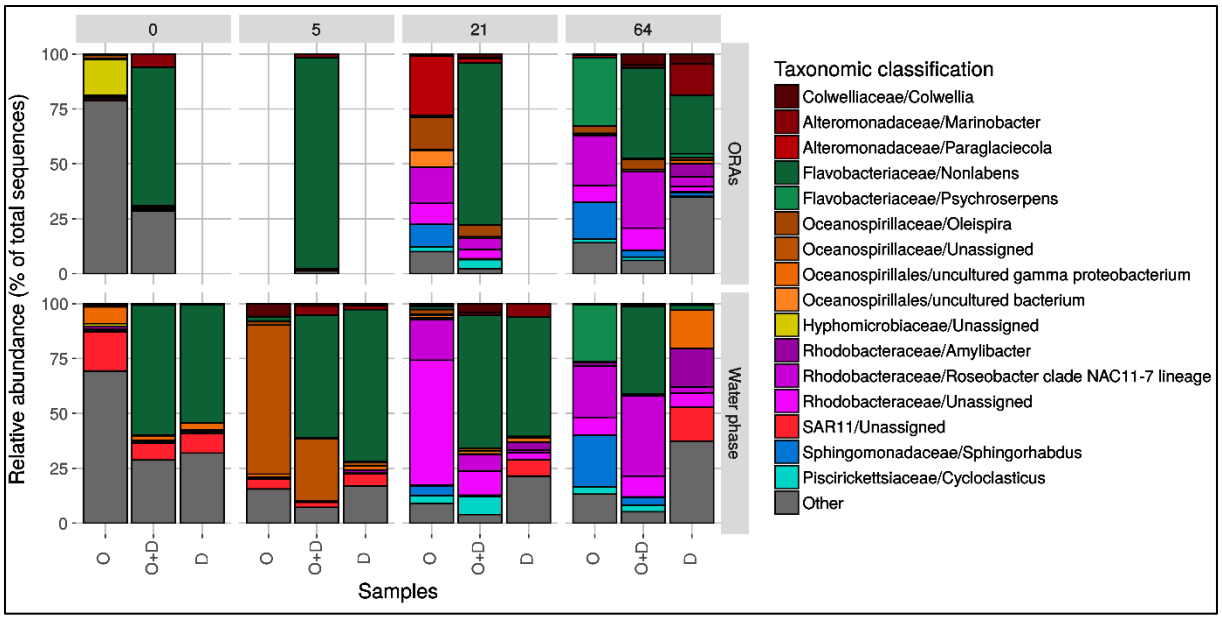

Fig. 5: *Bacterial community composition at family and genus level, except for Oceanospirillales and SAR11, that were only identified at order level. Results are based on 16S amplicon sequencing of ORAs and corresponding water phases derived DNA from O+D- (oil + diatoms) samples, O- (oil) samples and D- (diatoms) samples at individual sampling days. The relative abundance of taxa present at > 5% is derived from three independent biological replica from microcosm experiments.*

Supplementary Data

Click here to download Supplementary Data: Supplementary_rev.docx

Supplementary Data

Click here to download Supplementary Data: Supplementary table Tab. S1.xlsx